Open Access Full Text Article

ORIGINAL RESEARCH

Prognostic and Predictive Value of a 15 Transcription Factors (TFs) Panel for Hepatocellular Carcinoma

Tian-Hao Zhou[1],*
Jing-Zhi Su[2],*
Rui Qin[3]
Xi Chen[4]
Gao-Da Ju[5]
Sen Miao[3]

[1]Shanghai First People's Hospital, Shanghai Jiao Tong University School of Medicine, Shanghai 200080, People's Republic of China; [2]Department of Anatomy and Neurobiology, School of Basic Medical Science, Central South University, Changsha, Hunan, People's Republic of China; [3]Department of Pathology, Affiliated Hospital of Jining Medical University, Jining 272000, People's Republic of China; [4]Department of Internal Medicine, Qilu Hospital of Shandong University, Jinan 250000, People's Republic of China; [5]Department of Oncology, Beijing Cancer Hospital, Peking University, Beijing 102206, People's Republic of China

*These authors contributed equally to this work

Correspondence: Sen Miao
Department of Pathology, Affiliated Hospital of Jining Medical University, Jining 272000, People's Republic of China
Email miaosen128@163.com

Gao-Da Ju
Department of Oncology, Beijing Cancer Hospital, Peking University, Beijing 102206, People's Republic of China
Email jgd0412@163.com

Purpose: Hepatocellular carcinoma (HCC) is one of the most devastating diseases worldwide. Limited performance of clinicopathologic parameters as prognostic factors underscores more accurate and effective biomarkers for high-confidence prognosis that guide decision-making for optimal treatment of HCC. The aim of the present study was to establish a novel panel to improve prognosis prediction of HCC patients, with a particular interest in transcription factors (TFs).

Materials and Methods: A TF-related prognosis model of liver cancer with data from ICGC-LIRP-JI cohort successively were processed by univariate and multivariate Cox regression analysis. Then, for evaluating the prognostic prediction value of the model, receiver operating characteristic (ROC) curve and survival analysis were performed both with internal data from the International Cancer Genome Consortium (ICGC) and external data from The Cancer Genome Atlas (TCGA). Furthermore, we verified the expression of three genes in HCC cell lines by Western blot and qPCR and protein expression level by IHC in liver cancer patients' sample. Finally, we constructed a TF clinical characteristics nomogram to furtherly predict liver cancer patient survival probability with TCGA cohort.

Results: By Cox regression analysis, a panel of 15 TFs (*ZNF331*, *MYCN*, *AHRR*, *LEF1*, *ZNF780A*, *POU1F1*, *DLX5*, *ZNF775*, *PLSCR1*, *FOXK1*, *TAL2*, *ZNF558*, *SOX9*, *TCFL5*, *GSC*) was identified to present with powerful predictive performance for overall survival of HCC patients based on internal ICGC cohort and external TCGA cohort. A nomogram that integrates these factors was established, allowing efficient prediction of survival probabilities and displaying higher clinical utility.

Conclusion: The 15-TF panel is an independent prognostic factor for HCC, and 15 TF-based nomogram might provide implication an effective approach for HCC patient management and treatment.

Keywords: hepatocellular carcinoma, prognosis, transcription factor, overall survival

Introduction

Hepatocellular carcinoma (HCC), the most frequently diagnosed malignancy, ranks the third leading cause of cancer-related deaths worldwide,[1–3] notorious for its poor prognosis. Despite surgical interventions and other treatments such as targeted therapies and immunotherapy, the five-year survival rate for HCC remains less than 20%. Prognostic assessment is of clinical significance to guide decision-making for optimal treatment of HCC patients. Although the clinical outcome of patients with HCC is primarily correlated with risk factors including TNM staging, metastasis, tumor size, and circulating AFP levels,[4] these

currently used evaluation indicators cannot enable accurate and individualized prognostic information to facilitate effective therapeutic options. It is therefore important to investigate the effective prognostic predictors affecting overall survival (OS).

The human genome is predicted to encode over 2000 transcription factors (TFs), which integrate distinct signals to coordinate specific gene expression programs implicated in multiple cellular processes including tumorigenesis.[5] It has been well-established that TFs are commonly deregulated in many human cancer types such as liver cancer.[6,7] The remarkable diversity and potency of TFs as drivers for tumor initiation and disease progression render them attractive prognostic as well as therapeutic targets for cancers.[8–10] In spite of accumulating studies with regard to prognostic ability of individual factors that have been reported, effective biomarkers in clinical setting are lacking.

In our study, we performed a systematic data-dependent bioinformatic analysis to identify high-confidence master TFs related to prognosis of liver cancer patients, and established a nomogram that integrated a novel panel of six TFs (*LEF1*, *ZNF775*, *FOXK1*, *SOX9*, *TCFL5* and *GSC*) capable of presenting strong ability in predicting overall survival of HCC patients.

Materials and Methods
Data Acquisition
The ICGC-LIRP-JI cohort was downloaded from HCCDB database (http://lifeome.net/database/hccdb/home.html).[11] The TCGA-LIHC-FPKM cohort was downloaded from The Cancer Genomic Atlas (TCGA) website (https://portal.gdc.cancer.gov/). The unit of expression matrix from TCGA cohort was transferred from FPKM to TPM by R software. The TF list was downloaded from the Human Transcription Factors website (http://humantfs.ccbr.utoronto.ca/).[12]

Constructed and Validated a TF-related Prognostic Model of HCC Patients
The tumor samples with survival information were extracted from the ICGC-LIRP-JI cohort and were utilized to constructed a TF-related prognostic model of HCC patients. Univariate and multivariate Cox risk regression analyses were successively performed to

identify TFs significantly related to the prognosis of HCC patients. To validate the prognostic prediction value of the model, ROC curve analysis[13] and survival analysis were performed by R software with data form both ICHC and TCGA cohort. Finally, by utilizing the clinical information from the TCGA cohort, we constructed and validated a TFs clinical-character istics nomogram of HCC patients.

Identified and Validated Differentially Expressed TFs (DETFs) in a Model Between HCC and Adjacent Normal Liver Tissues
The R package "limma"[14] was used to identify DETFs with |log2FC| >1 and FDR <0.05 in the TCGA cohort or |log2FC| >0.4 and FDR <0.05 in the ICGC cohort. The Human Protein Atlas (HPA) database (http://www.proteinatlas.org) was utilized to validated the protein expression of DETFs between liver carcinoma and normal liver tissues.[15,16] Besides, qPCR and Western blot were utilized to examine the expression of DETFs in human normal liver cell and liver cancer cell lines.

Cell Cultures
Human liver cancer cell lines HepG3B, SMMC-7721, Huh7 and human normal liver cell line L-02 were obtained from ATCC and cultivated in DMEM medium (Gibco, USA) supplemented with 1% penicillin-streptomycin solution (Procell, China) and 10% fetal bovine serum (Gibco, USA) at 37°C with 5% CO_2.

Western Blotting Analysis
Cellular total proteins were extracted by denatured lysis buffer and then quantified by pierce BCA protein assay (Thermo Scientific, USA). 20 μg total protein loaded in SDS-PAGE were separated on SDS-PAGE, transferred to NC membranes (Millipore, USA), blocked, then detected by primary antibody followed by HRP-conjugated secondary antibody (Sigma, USA), and then detected by enhanced chemiluminescence (ECL). Antibodies against *FOXK1* (1:2000, A15220) and *β-Actin* (1:10,000, AC026) were obtained from ABclonal (Hubei, China). Antibodies against *GSC* (1:1000, ab109024) was purchased from Abcam (Shanghai, China). Antibodies against *ZNF775* (1:1000,

qPCR Analysis

Total RNA was isolated from cells by utilizing TRIzol reagent (Invitrogen). cDNA was obtained by utilizing Primer Script RT reagent Kit (Takara). The qPCR reaction was performed according to the operating instructions of the SYBR Green (Toyobo Co., Ltd, Japan). The expression of β-Actin was considered as internal control. The 2-ΔΔCT method was utilized to compared the mRNA expression of genes between L-02 and HepG3B, SMMC-7721, Huh7. The primers used in this study for qPCR reaction are designed by NCBI, and all are exon spanning and shown below: *FOXK1* (NM_001037165.2) primer F: 5′-GCTCCTCCAGTTACCG CTTT-3′, primer R: 5′-GACTCATCCTTGGGGCTGTC-3′; *GSC* (NM_173849.3) primer F: 5′-GCGAGGAGAAAGT GGAGGTC-3′, primer R: 5′-CCTCTTCCCTCTTCTCCG GT-3′; *ZNF775* (NM_173680.4) primer F: 5′-GACAGG AGGAGTCTGGGAGT-3′, primer R: 5′-CCGCAGTCCA GGCATACAAA-3′; internal control gene *β-Actin* (NM_00 1101.5) primer F:5′-GCACTCTTCCAGCCTTCCTT-3′, primer R: 5′-AATGCCAGGGTACATGGTGG-3′.

Human HCC Sample Collection

All the human HCC samples were collected from the Affiliated Hospital of Jining Medical University. The experiment with human tissues was authorized by the Human Ethics Committee of Jining Medical University. All subjects provided written informed consent.

IHC Analysis

Paraffin-embedded tissues were cut into 3-μm sections. IHC signals were developed using antibodies against human *FOXK1* (1:500, PA5-81177) was purchased from Thermo Fisher Scientific (Shanghai, China), *GSC* (1:400, TA500023), and *ZNF775* (1:300, orb318036) were purchased from Biorbyt (Shanghai, China). Primary antibodies were incubated overnight at 4°C. IHC score were according to the following roles: positive reactions were defined as those showing brown signals in the cell nuclear. For *FOXK1*, *GSC* and *ZNF775*, a staining index (values, 0–12) was determined by multiplying the score for staining intensity with the score for positive area. Staining intensity grade is classified as: 0, negative; 1, weak; 2, moderate; 3, strong. The frequency of positive cells was defined as: less than 5%, 0 point; 5–25%, 1 point; 26–50%, two points; 51%–75%, 3 points; more than 75%, 4 points.

Statistical Analysis

All data were statistically analyzed with GraphPad Prism 8.0. Two-tailed *t* test was utilized to analyze the difference between the two groups. Pearson's test was applied to determine the correlation
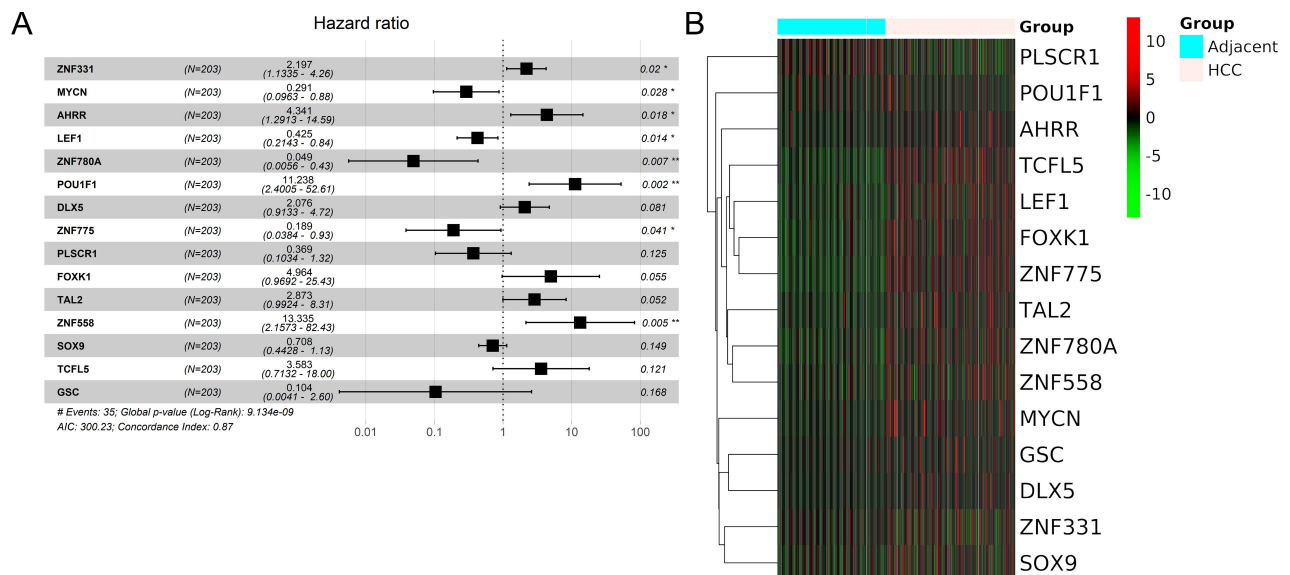
Figure I A panel of 15 TFs was identified to have predictive value based on the ICGC cohort. (**A**) Multivariate Cox regression analysis revealed that 15 TFs were independent indicators for HCC prognosis. (**B**) Heat map analysis of the mRNA expression of 15 TFs in liver cancer tissues and adjacent liver tissues based on the ICGC cohort. *P<0.05, **P<0.01.

between clinicopathological parameters and protein expression. Data were presented as mean±SD or SEM. Differences at $P<0.05$ were considered statistically significant.

Results
Construct TF-related Prognostic Model of HCC

In this study, to investigate the prognostic utility of TFs for HCC, we extracted mRNA expression matrix of 203 HCC samples accompanied with their survival information from the ICGC-LIRP-JI cohort. By performing univariate Cox regression analysis, 29 TFs were considered as significant prognostic marker of HCC patients ($P<0.05$). Then, these 29 candidate prognostic TFs were selected for further multivariate Cox regression analysis. To this end, 15 TFs including *ZNF331*, *MYCN*, *AHRR*, *LEF1*, *ZNF780A*, *POU1F1*, *DLX5*, *ZNF775*, *PLSCR1*, *FOXK1*, *TAL2*, *ZNF558*, *SOX9*, *TCFL5*, *GSC* were identified to be independent indicators for patient survival ([Figure 1A](#)). Consistently, this finding was supported by publicly available datasets of the ICGC-LIRP-JI cohort showing that the expression of the 15 TFs were remarkably deregulated in liver cancerous tissues compared with adjacent normal liver tissues ([Figure 1B](#)).
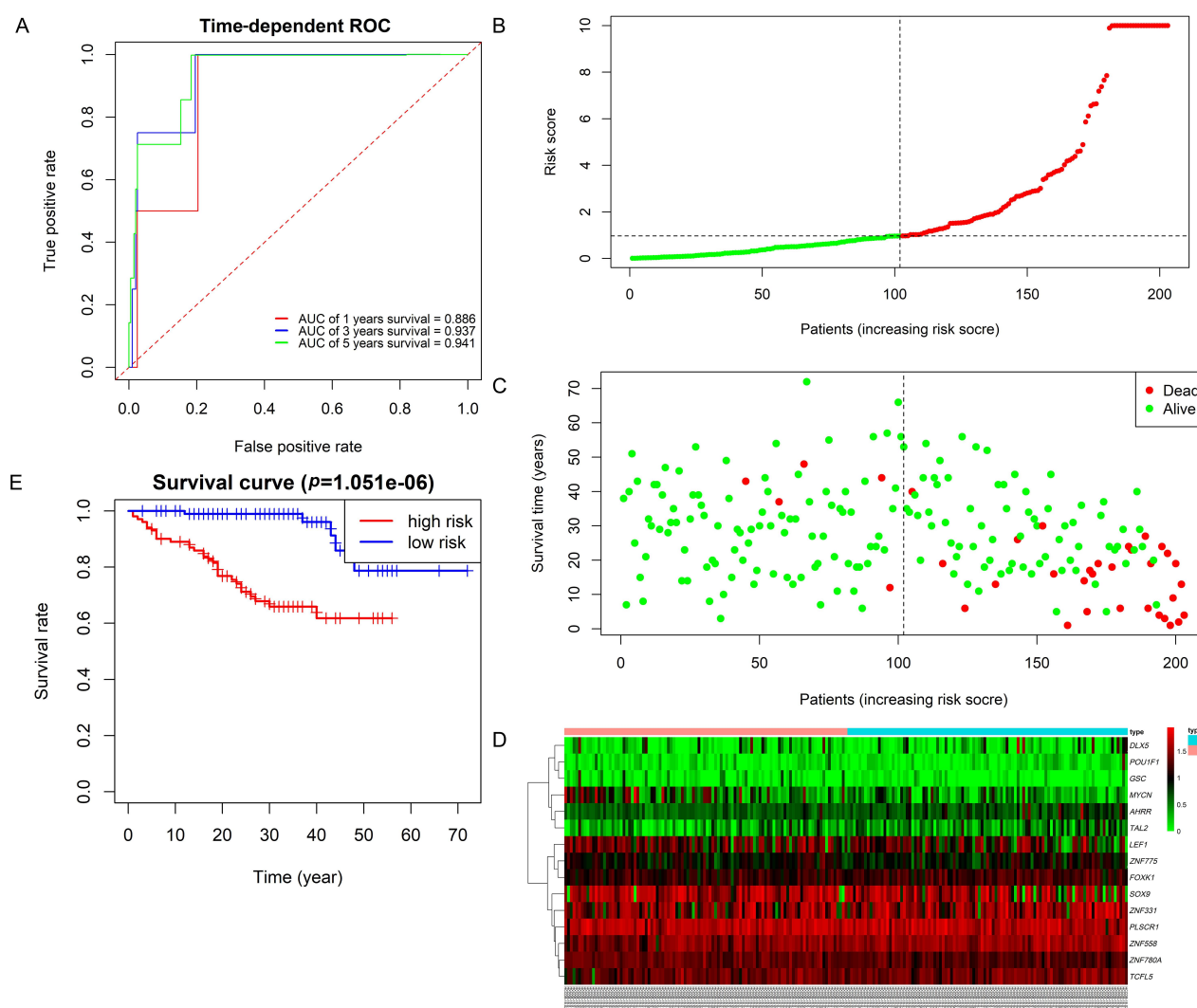
Figure 2 A 15 TF stratified overall survival rate in patients with HCC in internal cohort. (**A**) Time-dependent receiver operating characteristic curves of a 15 TFs. (**B**) Risk score distribution of patients with HCC. (**C**) Demonstration of survival status of patients with HCC. (**D**) Expression of 15 TFs in HCC patients by heat map analysis. (**E**) Kaplan–Meier survival curves for overall survival rate. The patients were then divided into high-risk internal group and low-risk internal group by the cutoff value of median risk score.
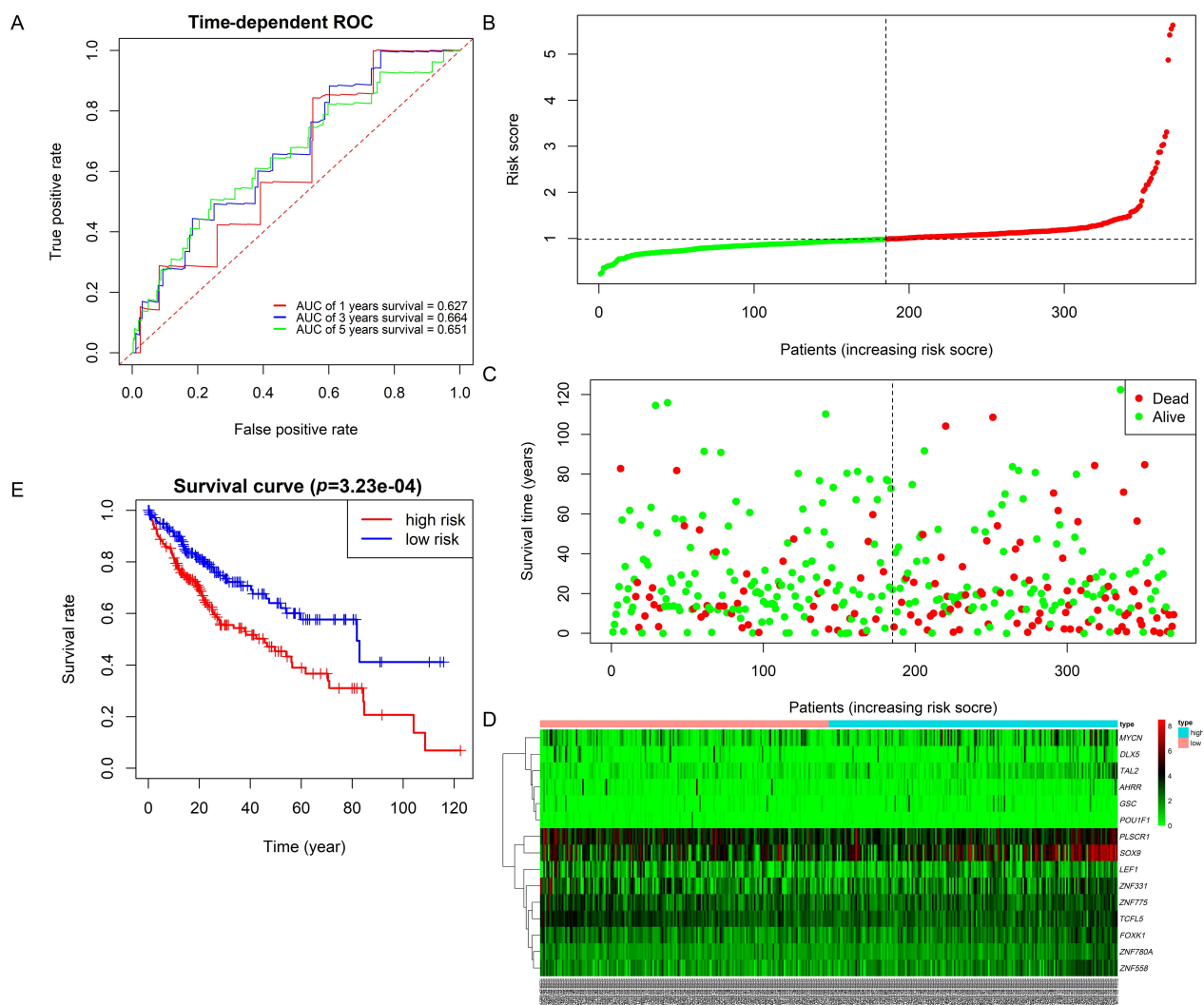**Abbreviations:** ROC, receiver operating characteristic curves; AUC, area under the curve.

Validate TF-related Prognostic Model of HCC

To validate the prognostic performance of the 15 TFs panel, the ICGC-LIRP-JI cohort was used as internal validation group, and the TCGA cohort was regarded as external validation group for ROC curve and survival analysis. The risk score of each sample was calculated by R software. In the internal validation group, our result showed that the area under the ROC curve (AUC) of one-year survival, three-year survival and five-year survival were 0.886, 0.937, and 0.941, respectively (Figure 2A). The patients were then divided into two groups (high-risk internal group and low-risk internal group) by the cutoff value of median risk score. The expression heat map, survival status of HCC patients, and the signature of risk score with respect to the 15 TFs in the low-risk internal and high-risk internal groups were showed in Figure 2B–D. Furthermore, we performed Kaplan–Meier plot to analyze different survival times between the high-risk internal group and low-risk internal group. The result indicated that HCC patients of the low-risk internal group had longer overall survival than those of the high-risk internal group (Figure 2E). In addition, we evaluated the sensitivity and specificity of the TF-related prognostic model of HCC in external validation group.

Figure 3 Validation of the 15 TF prognostic model of HCC patients in the external cohort. (**A**) Time-dependent receiver operating characteristic curves of 15 TFs in the external cohort. (**B**) Risk score distribution of patients with HCC. (**C**) Demonstration of survival status of patients with HCC. (**D**) Expression of 15 TFs in HCC patients by heat map analysis. (**E**) Kaplan–Meier survival curves for overall survival rate. The patients were then divided into high-risk internal group and low-risk internal group by the cutoff value of median risk score.
Abbreviations: ROC, receiver operating characteristic curve; AUC, area under the curve.

Although ROC curve analysis show that a moderately prognostic prediction value, with AUC values of one, three, and five years were 0.627, 0.664, and 0.651 (Figure 3A). However, the patients in the low-risk external group were associated with favorable clinical outcome in contrast to those in the high-risk external group, suggesting the consistency between internal and external validation groups (Figure 3B–E). Thus, the 15 TFs panel enables promising predictive power for patients with liver cancer. We next constructed a TF-related prognostic nomogram for predicting HCC patient survival probability (Figure 4).

Validate the Expression of DETFs in a Model Between Normal Liver Cell and Liver Cancer Cell Lines

By integration and cross-reference between HCC and normal liver tissues both in ICGC and TCGA cohorts, we identified six DETFs between HCC and normal liver tissues in both ICGC and TCGA cohorts (Figure 5A). To provide experimental evidence, three of the six

DETFs were selected for further validation. Indeed, the protein expression of the three TFs (*SOX9*, *TCFL5*, *LRF1*) were higher in liver carcinoma than in normal liver tissues, as revealed by IHC analysis in the HPA database (Figure 5B). In addition, qPCR as well as Western blotting analysis indicated that HCC cell lines including HepG3B, SMMC-7721, Huh7 displayed higher expression of *FOXK1*, *GSC* and *ZNF775* compared to human normal liver cell L-02 (Figure 5C and D). Furthermore, we verified expressions of *FOXK1*, *GSC* and *ZNF775* in 15 HCC cancer and paired adjacent normal liver tissues. *FOXK1*, *GSC* and *ZNF775* were all significantly higher expressed in tumor tissue than normal liver tissue (Figure 5E).

TF Panel was Significantly Correlated with Clinical Characteristics and Predicted Prognosis of HCC Patients

For evaluating prognostic capacity of the panel of 15 TFs, 370 HCC cases with complete clinical information were extracted to establish the prognostic model. The
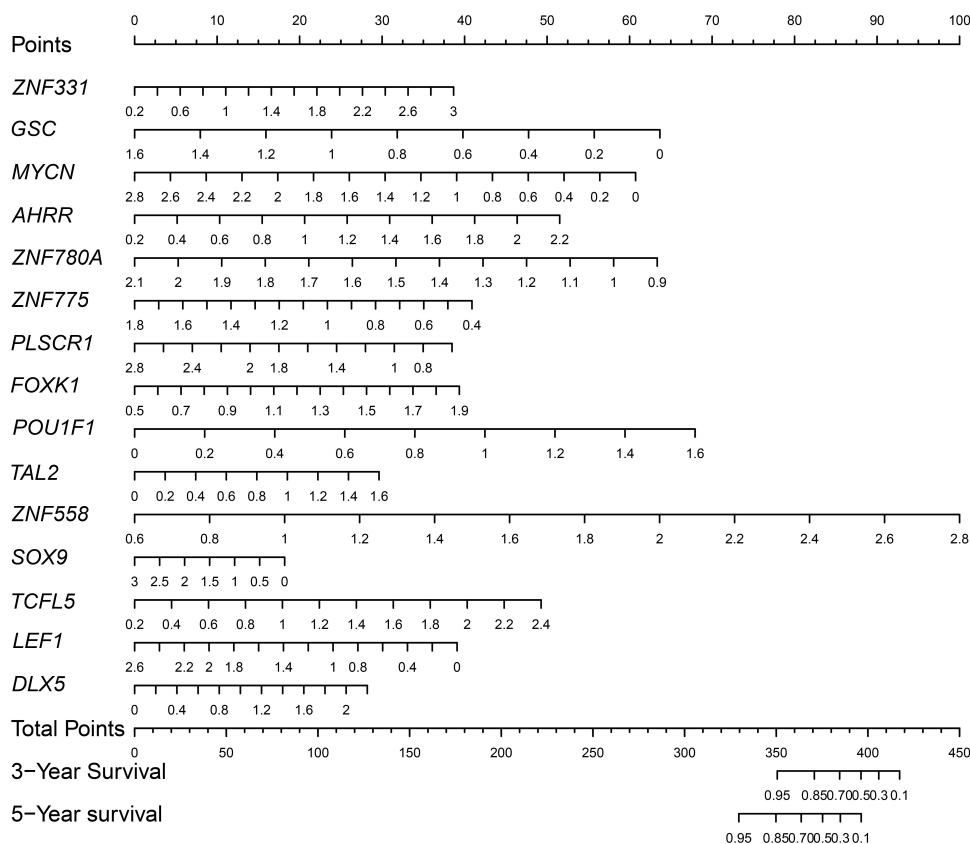
Figure 4 Nomogram analysis for overall survival in patients with HCC. A nomogram was developed based on the independent risk factors identified in the multivariate analysis.
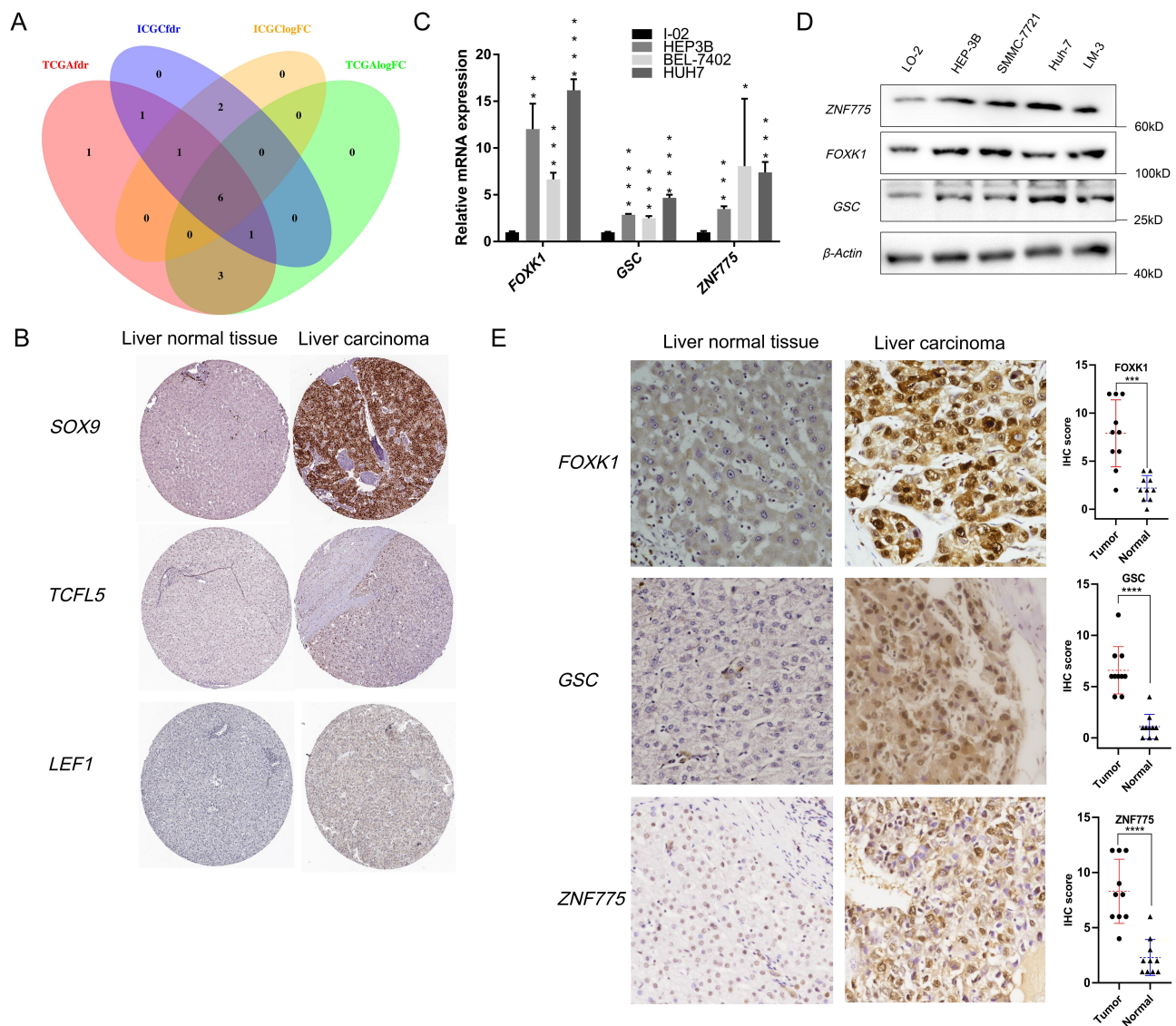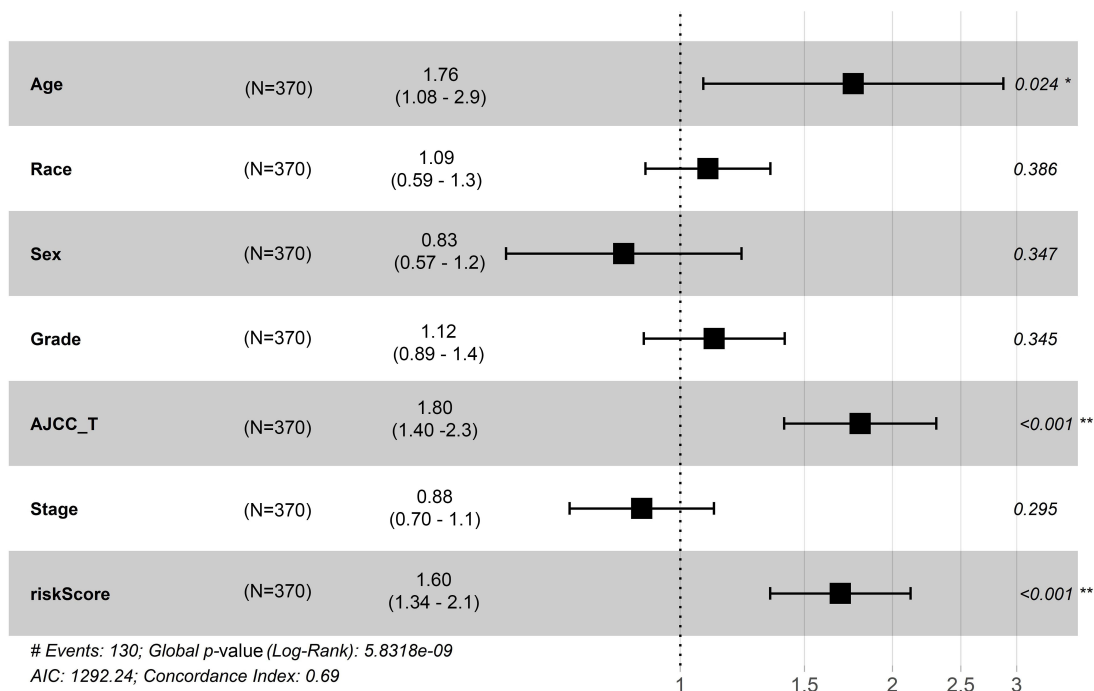
Figure 5 Screening and validation of six DETFs in the ICGC and TCGA cohorts. (**A**) A Venn diagram showed six DETFs between HCC and normal liver tissues both in the ICGC and TCGA cohorts. (**B**) IHC analysis of *SOX9*, *TCFL5* and *LEF1* HCC and normal liver tissues. Representative IHC images were showed. (**C**) Quantitative PCR analysis of *FOXK1*, *GSC* and *ZNF775* transcripts in HCC cell lines. (**D**) Determination of *FOXK1*, *GSC* and *ZNF775* expressions by Western blotting in in HCC cell lines. (**E**) Representative cases showed the upregulation of *FOXK1*, *GSC,* and *ZNF775* protein in HCC when compared to its adjacent normal liver. Semiquantitative analyses of IHC staining of *FOXK1*, *GSC* and *ZNF775* in 15 HCC patients column with tumor sample and adjacent normal liver tissue. *$P<0.05$, **$P<0.01$, ***$P<0.001$, ****$P<0.0001$.

multivariate Cox regression analysis suggested that age, AJCC_T and TF-related risk scores were independent prognostic factors for HCC patients (Figure 6A). Then, a nomogram was constructed (Figure 6B). The ROC curve analysis of the prognostic model composed of clinical characteristics and TF risk scores showed a better AUC of five-year survival value than only by 15 TFs in the TCGA cohort (Figure 7A). Similarly, in clinical and TF models, HCC patients in the high risk group had poorer OS than in the low risk group (Figure
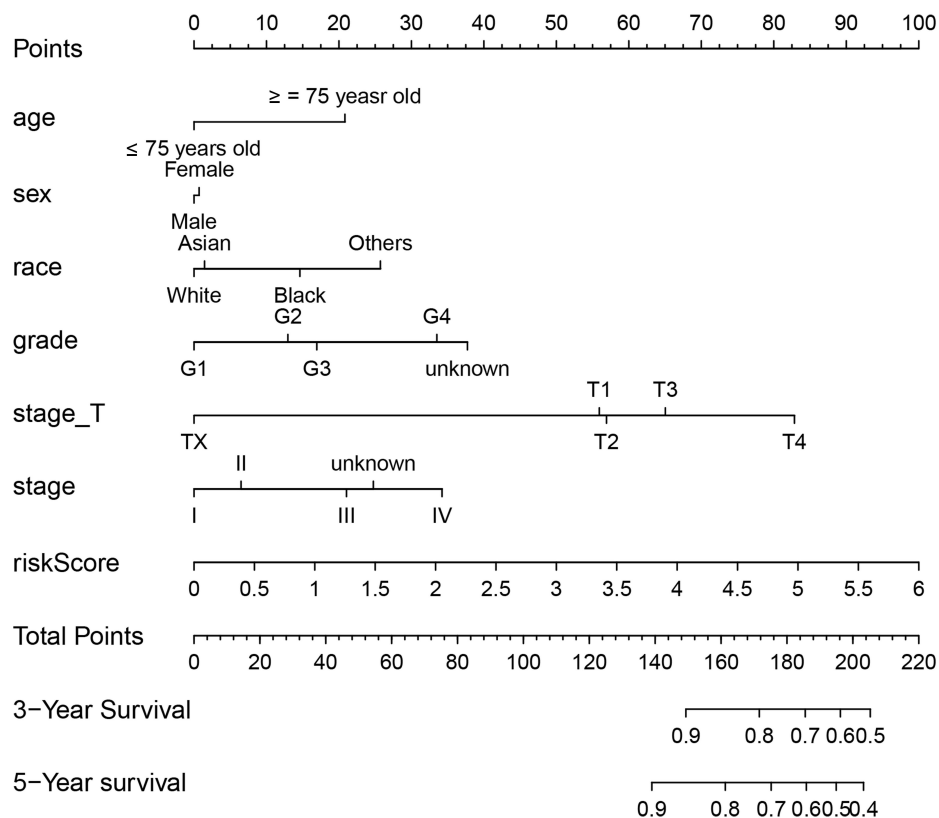
7B). In addition, the calibration curve for three-year survival and five-year survival showed a consistency between predicted value of model and actual observed value (Figure 7D). Finally, we performed Kaplan–Meier survival analysis of patients with HCC based on each clinical characteristic independently. The result indicated that age, AJCC_T stage and TNM stage were significantly correlated with survival of HCC patients ($p<0.05$) (Figure 8A–C) while grade, race, and gender were not (Figure 8D–E).

A

Hazard ratio

Age	(N=370)	1.76 (1.08 - 2.9)		0.024 *
Race	(N=370)	1.09 (0.59 - 1.3)		0.386
Sex	(N=370)	0.83 (0.57 - 1.2)		0.347
Grade	(N=370)	1.12 (0.89 - 1.4)		0.345
AJCC_T	(N=370)	1.80 (1.40 -2.3)		<0.001 **
Stage	(N=370)	0.88 (0.70 - 1.1)		0.295
riskScore	(N=370)	1.60 (1.34 - 2.1)		<0.001 **

 # Events: 130; Global p-value (Log-Rank): 5.8318e-09
AIC: 1292.24; Concordance Index: 0.69

1   1.5   2   2.5   3

B

Points
0   10   20   30   40   50   60   70   80   90   100

age
≥ = 75 yeasr old
≤ 75 years old

sex
Female
Male

race
Asian   Others
White   Black

grade
G2   G4
G1   G3   unknown

stage_T
T1   T3
TX   T2   T4

stage
II   unknown
I   III   IV

riskScore
0   0.5   1   1.5   2   2.5   3   3.5   4   4.5   5   5.5   6

Total Points
0   20   40   60   80   100   120   140   160   180   200   220

3−Year Survival
0.9   0.8   0.7 0.60.5

5−Year survival
0.9   0.8   0.7 0.60.50.4

Figure 6 Prognostic capacity evaluation and nomogram analysis of panel of 15 TFs of HCC patients. (**A**) Evaluation of prognostic capacity of indicated clinical parameters. (**B**) A nomogram was developed based on the independent risk factors identified in the multivariate analysis. *P<0.05, **P<0.001.
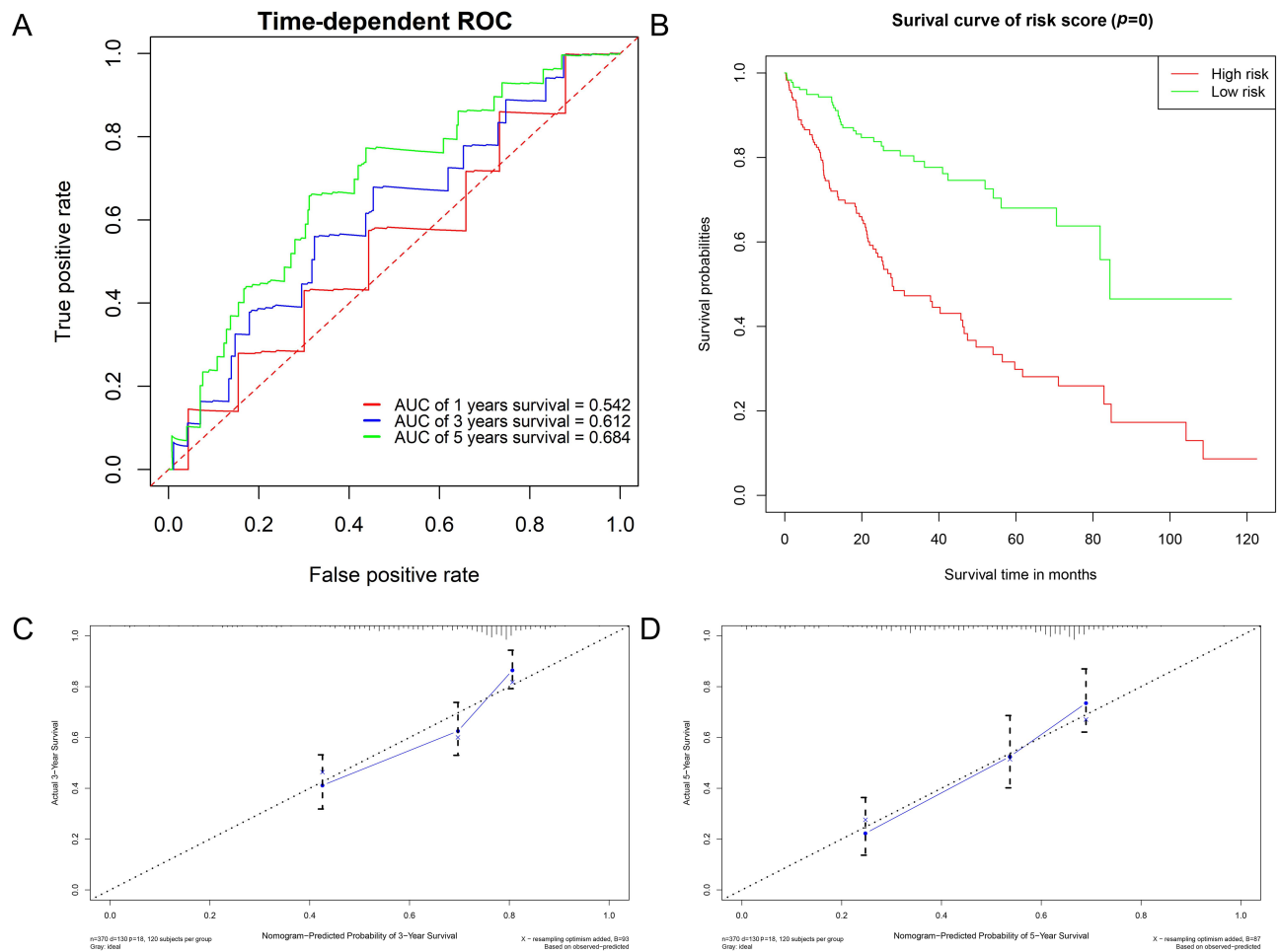
Figure 7 Validation of TF combined clinical parameters prognostic model of HCC patients in the external cohort. (**A**) Time-dependent receiver operating characteristic curves of TFs and clinical parameters in the TCGA cohort. (**B**) Kaplan–Meier survival curves for overall survival rate. The patients were then divided into high-risk group and low-risk group by the cutoff value of median risk score. (**C**) Calibration plots of three-year survival of TFs combined clinical parameters model in the TCGA cohort. (**D**) Calibration plots of 5five-year survival of TFs combined clinical parameters model in the TCGA cohort.
Abbreviations: ROC, receiver operating characteristic curve; AUC, area under the curve.

Discussion

Over the past decades, multiple studies found that TFs are frequently implicated in the tumor initiation, disease progression, and tumor relapse of many human cancers including HCC.[5–7] For instance, nuclear factor-κB (NF-κB), a critical regulator of innate immunity, was considered to be a driver in tumorigenesis of HCC and a potential drug target for treating HCC.[17] Besides, it was reported that HCC patients with overexpression of signal transducer and activator of transcription 3 (*STAT3*) have shorter survival compared to patients with low expression of *STAT3*.[18] These studies confirmed the association between TFs and HCC, indicating that the probability of TFs for predicting the survival outcomes of HCC patients.

In this study, we identified a panel of 15 TFs (*ZNF331, MYCN, AHRR, LEF1, ZNF780A, POU1F1, DLX5,*

*ZNF775, PLSCR1, FOXK1, TAL2, ZNF558, SOX9, TCFL5, GSC*) that was capable of predicting HCC in the internal ICGC cohort and external TCGA cohort. We further confirmed that six TFs in the model (*LEF1, ZNF775, FOXK1, SOX9, TCFL5,* and *GSC*) overexpressed in HCC and might be implicated in the occurrence and progression of carcinoma. The study design is illustrated in Figure 9.

It is reported that *GSC* plays an important role in metastases of breast cancer and HCC through initiating epithelial-mesenchymal transition (EMT) process and the expression level of *GSC* is negatively correlated with the survival of HCC patients.[19–21] Forkhead box K1 (*FOXK1*) is a key TF involved in initiation of cancer, such as HCC, gastric cancer, colorectal cancer, prostate cancer and esophageal cancer.[22–26] Although
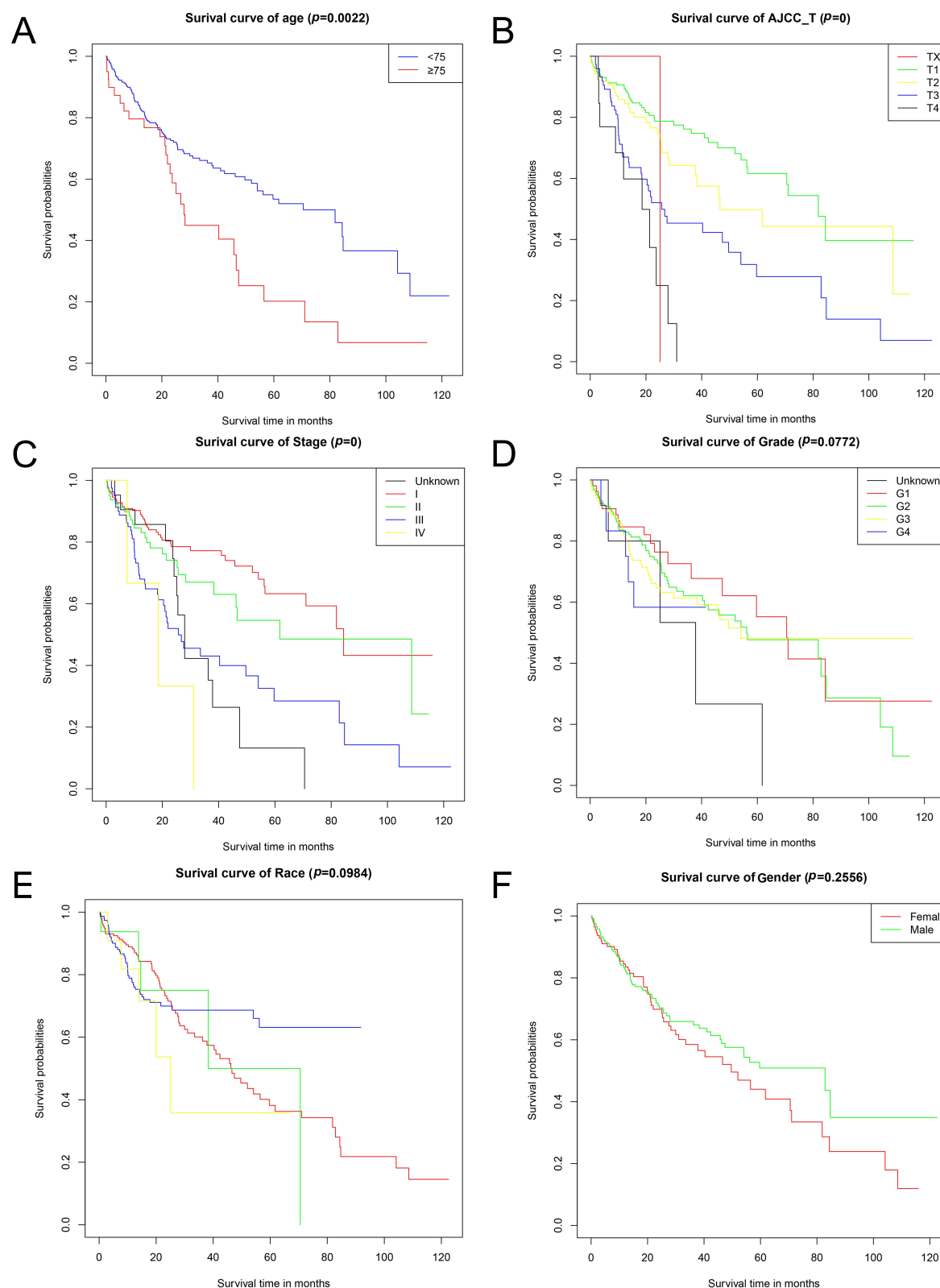
Figure 8 Survival analysis of clinical parameters in HCC patients. Kaplan–Meier survival curves for overall survival rate. (**A**) Age. (**B**) AJCC_T. (**C**) Stage. (**D**) Grade. (**E**) Race. (**F**) Sex.
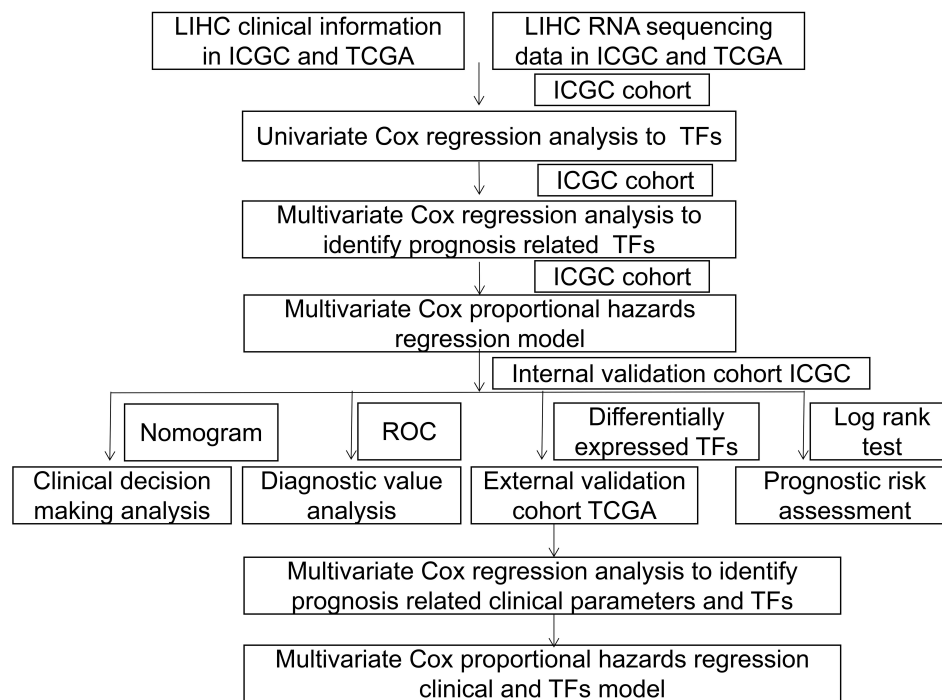
Figure 9 Whole procedure for analyzing TFs in HCC.

FOXK1 is overexpressed in many tumor tissues,[23,24,26] it is still unclear whether *FOXK1* is associated with the prognosis of liver cancer patients. However, in this study, our model revealed that *FOXK1* might play a great role in predicting prognosis of HCC patients. In addition, few reports described the correlation between cancers and *ZNF775*. Our study firstly confirmed that the expression of *ZNF775* was higher in the liver cancer cells than normal liver cells. Furthermore, we found that *ZNF775* could be a prognostic prediction marker for liver cancer patients. Lymphoid enhancer-binding factor-1 (*LEF1*) is closely related to prognosis of HCC patients.[27] Many studies found that *LEF1* is a TF regulating tumor stemness, growth, invasion, EMT, and metastasis of HCC by activating Wnt/β-catenin signaling and NOTCH signaling.[27–31] Our study confirmed *LEF1* overexpression in HCC, and could serve as an excellent prognostic prediction marker of HCC patients. As a TF, sex determining region Y-box 9 (*SOX9*) is a well-established cancer stem cell (CSC) marker of HCC, and promotes the stemness property of of HCC by initiating Wnt/β-catenin pathway.[32,33] It is reported that the inhibition of *SOX9* decreased the proliferation, invasion and metastasis of HCC.[34,35] In addition, our study is consistent with the previous study[36] that HCC patients with

overexpression of *SOX9* has a poorer survival prognosis. In a previous study, researchers found that *TCFL5* was overexpressed in carcinomas than normal tissues[37] and promoted the tumorigenesis, cell viability, and growth of colorectal carcinoma.[38] Nevertheless, limited evidence is provided. Our study confirmed that *TCFL5* was overexpressed in liver carcinoma tissues compared to normal liver tissues, indicating that *TCFL5* plays a great role in constructing prognostic model of HCC patients.

Although we successfully constructed and validated a TF-related prognostic model that may contribute to guide clinicians to predict the prognosis of HCC patients, there were still some limitations in our study. Firstly, the ROC curve revealed that AUC for three- or five-year survival in the TCGA cohort were not up to 0.9. However, in general, the AUC ≥0.9 meant a strong prognostic value. Secondly, there was a need for more molecular mechanism research to further consolidate our result. Nevertheless, the defects cannot obscure the virtues; our study firstly explored the correlation of TFs and prognosis of HCC patients in detail. In addition, our 15 TF-related prognostic model validated by data from both the internal and external cohort. Besides, for predicting prognosis of HCC patients, it would be better to combine the 15 TF-related model with clinical characteristics, such as age and tumor size.

Author Contributions

Miao and Ju conceived and supervised the study; Zhou and Su analyzed the data and wrote the manuscript; Chen conducted the follow-ups and collected the data; all authors read and approved the manuscript. All authors made substantial contributions to conception and design, acquisition of data, or analysis and interpretation of data; took part in drafting the article or revising it critically for important intellectual content; agreed to submit to the current journal; gave final approval of the version to be published; and agree to be accountable for all aspects of the work.

Disclosure

The authors report no conflicts of interest in this work.

References

1. Globacon. *Fact Sheet: China*. World Health Organization; 2018.
2. Zhang Y, Liu Y, Duan J, et al. Hippocalcin-like 1 suppresses hepatocellular carcinoma progression by promoting p21(Waf/Cip1) stabilization by activating the ERK1/2-MAPK pathway. *Hepatology*. 2016;63:880–897.
3. Liu Y, Zhang Y, Wang S, et al. Prospero-related homeobox 1 drives angiogenesis of hepatocellular carcinoma through selectively activating interleukin-8 expression. *Hepatology*. 2017;66:1894–1909.
4. Bruix J, Reig M, Sherman M. Evidence-Based Diagnosis, Staging, and Treatment of Patients With Hepatocellular Carcinoma. *Gastroenterology*. 2016;150:835–853.
5. Bhagwat AS, Vakoc CR. Targeting Transcription Factors in Cancer. *Trends Cancer*. 2015;1:53–65.
6. Rey S, Schito L, Wouters BG, Eliasof S, Kerbel RS. Targeting Hypoxia-Inducible Factors for Antiangiogenic Cancer Therapy. *Trends Cancer*. 2017;3:529–541.
7. Heppler LN, Frank DA. Targeting Oncogenic Transcription Factors: therapeutic Implications of Endogenous STAT Inhibitors. *Trends Cancer*. 2017;3:816–827.
8. Luedde T, Beraza N, Kotsikoris V, et al. Deletion of NEMO/IKKgamma in liver parenchymal cells causes steatohepatitis and hepatocellular carcinoma. *Cancer Cell*. 2007;11:119–132.
9. Inokuchi S, Aoyama T, Miura K, et al. Disruption of TAK1 in hepatocytes causes hepatic injury, inflammation, fibrosis, and carcinogenesis. *Proc Natl Acad Sci U S A*. 2010;107:844–849.
10. Bettermann K, Vucur M, Haybaeck J, et al. TAK1 Suppresses a NEMO-Dependent but NF-κB-Independent Pathway to Liver Cancer. *Cancer Cell*. 2010;17(5):481–496. doi:10.1016/j.ccr.2010.03.021
11. Lian Q, Wang S, Zhang G, et al. HCCDB: A Database of Hepatocellular Carcinoma Expression Atlas. *Genomics Proteomics Bioinformatics*. 2018;16(4):269–275. doi:10.1016/j.gpb.2018.07.003
12. Lambert SA, Jolma A, Campitelli LF, et al. The Human Transcription Factors. *Cell*. 2018;172(4):650–665. doi:10.1016/j.cell.2018.01.029
13. Heagerty PJ, Lumley T, Pepe MS. Time-Dependent ROC Curves for Censored Survival Data and a Diagnostic Marker. *Biometrics*. 2000;56(2):337–344. doi:10.1111/j.0006-341X.2000.00337.x
14. Ritchie ME, Phipson B, Wu D, et al. limma powers differential expression analyses for RNA-sequencing and microarray studies. *Nucleic Acids Res*. 2015;43(7):e47. doi:10.1093/nar/gkv007
15. Uhlén M, Fagerberg L, Hallström BM, et al. Proteomics. *Tissue-Based Map Human Proteome Sci*. 2015;347:1260419.
16. Uhlen M, Zhang C, Lee S, et al. A pathology atlas of the human cancer transcriptome. *Science*. 2017;357.
17. Luedde T, Schwabe RF. NF-κB in the liver–linking injury, fibrosis and hepatocellular carcinoma. *Gastroenterol Hepatol (N Y)*. 2011;8:108–118.
18. Lee C, Cheung ST. STAT3: an Emerging Therapeutic Target for Hepatocellular Carcinoma. *Cancers*. 2019;11.
19. Niehrs C, Keller R, Cho KW, De Robertis EM. The homeobox gene goosecoid controls cell migration in Xenopus embryos. *Cell*. 1993;72:491–503.
20. Hartwell KA, Muir B, Reinhardt F, Carpenter AE, Sgroi DC, Weinberg RA. The Spemann organizer gene, Goosecoid, promotes tumor metastasis. *Proc Natl Acad Sci U S A*. 2006;103:18969–18974.
21. Xue T-C, Ge N-L, Zhang L, et al. Goosecoid promotes the metastasis of hepatocellular carcinoma by modulating the epithelial-mesenchymal transition. *PLoS One*. 2014;9:e109695.
22. Cui H, Gao Q, Zhang L, Han F, Wang L. Knockdown of FOXK1 suppresses liver cancer cell viability by inhibiting glycolysis. *Life Sci*. 2018;213:66–73.
23. Peng Y, Zhang P, Huang X, et al. Direct regulation of FOXK1 by C-jun promotes proliferation, invasion and metastasis in gastric cancer cells. *Cell Death Dis*. 2016;7:e2480.
24. Wu Y, Xie R, Liu X, et al. Knockdown of FOXK1 alone or in combination with apoptosis-inducing 5-FU inhibits cell growth in colorectal cancer. *Oncol Rep*. 2016;36:2151–2159.
25. Chen F, Xiong W, Dou K, Ran Q. Knockdown of FOXK1 Suppresses Proliferation, Migration, and Invasion in Prostate Cancer Cells. *Oncol Res*. 2017;25:1261–1267.
26. Chen D, Wang K, Li X, et al. FOXK1 plays an oncogenic role in the development of esophageal cancer. *Biochem Biophys Res Commun*. 2017;494:88–94.
27. Fang S, Liu M, Li L, et al. Lymphoid enhancer-binding factor-1 promotes stemness and poor differentiation of hepatocellular carcinoma by directly activating the NOTCH pathway. *Oncogene*. 2019;38:4061–4074.
28. Sun L, Liu T, Zhang S, Guo K, Liu Y. Oct4 induces EMT through LEF1/β-catenin dependent WNT signaling pathway in hepatocellular carcinoma. *Oncol Lett*. 2017;13:2599–2606.
29. Huang F-I, Chen Y-L, Chang C-N, Yuan R-H, Jeng Y-M. Hepatocyte growth factor activates Wnt pathway by transcriptional activation of LEF1 to facilitate tumor invasion. *Carcinogenesis*. 2012;33:1142–1148.
30. Zhang T, Ma Z, Liu L, et al. DDX39 promotes hepatocellular carcinoma growth and metastasis through activating Wnt/β-catenin pathway. *Cell Death Dis*. 2018;9:675.
31. Chen Y, Guo Y, Li Y, et al. miR-300 regulates tumor proliferation and metastasis by targeting lymphoid enhancer-binding factor 1 in hepatocellular carcinoma. *Int J Oncol*. 2019;54:1282–1294.
32. Kawai T, Yasuchika K, Ishii T, et al. SOX9 is a novel cancer stem cell marker surrogated by osteopontin in human hepatocellular carcinoma. *Sci Rep*. 2016;6:30489.
33. Richtig G, Aigelsreiter A, Schwarzenbacher D, et al. SOX9 is a proliferation and stem cell factor in hepatocellular carcinoma and possess widespread prognostic significance in different cancer types. *PLoS One*. 2017;12:e0187814.
34. Liu Y, Zhang W, Liu K, Liu S, Ji B, Wang Y. miR-138 suppresses cell proliferation and invasion by inhibiting SOX9 in hepatocellular carcinoma. *Am J Transl Res*. 2016;8:2159–2168.
35. Yan S, Shan X, Chen K, et al. LINC00052/miR-101-3p axis inhibits cell proliferation and metastasis by targeting SOX9 in hepatocellular carcinoma. *Gene*. 2018;679:138–149.
36. Guo X, Xiong L, Sun T, et al. Expression features of SOX9 associate with tumor progression and poor prognosis of hepatocellular carcinoma. *Diagn Pathol*. 2012;7:44.

37. Carvalho B, Postma C, Mongera S, et al. Multiple putative oncogenes at the chromosome 20q amplicon contribute to colorectal adenoma to carcinoma progression. *Gut*. 2009;58:79–89.

38. Sillars-Hardebol AH, Carvalho B, Tijssen M, et al. TPX2 and AURKA promote 20q amplicon-driven colorectal adenoma to carcinoma progression. *Gut*. 2012;61:1568–1575.